ELSEVIER

Deep-Sea Research II 52 (2005) 3281–3302

DEEP-SEA RESEARCH
PART II

www.elsevier.com/locate/dsr2

Sediment transport by sea ice in the Chukchi and Beaufort Seas: Increasing importance due to changing ice conditions?

H. Eicken[a,*], R. Gradinger[b], A. Gaylord[c], A. Mahoney[a], I. Rigor[d], H. Melling[e]

[a]*Geophysical Institute, University of Alaska Fairbanks, Fairbanks, AK 99775-7320, USA*
[b]*Institute of Marine Science, University of Alaska Fairbanks, Fairbanks, AK 99775-7230, USA*
[c]*Nuna Technologies, Homer, AK 99603, USA*
[d]*Applied Physics Laboratory, University of Washington, Seattle, WA 98105-6698, USA*
[e]*Institute of Ocean Sciences, P.O. Box 6000, Sidney, BC, Canada V8L 4B2*

Received 29 March 2004
Available online 28 November 2005

Abstract

Sediment-laden sea ice is widespread over the shallow, wide Siberian Arctic shelves, with off-shelf export from the Laptev and East Siberian Seas contributing substantially to the Arctic Ocean's sediment budget. By contrast, the North American shelves, owing to their narrow width and greater water depths, have not been deemed as important for basin-wide sediment transport by sea ice. Observations over the Chukchi and Beaufort shelves in 2001/02 revealed the widespread occurrence of sediment-laden ice over an area of more than 100,000 km^2 between 68 and 74°N and 155 and 170°W. Ice stratigraphic studies indicate that sediment inclusions were associated with entrainment of frazil ice into deformed, multiple layers of rafted nilas, indicative of a flaw-lead environment adjacent to the landfast ice of the Chukchi and Beaufort Seas. This is corroborated by buoy trajectories and satellite imagery indicating entrainment in a coastal polynya in the eastern Chukchi Sea in February of 2002 as well as formation of sediment-laden ice along the Beaufort Sea coast as far eastward as the Mackenzie shelf. Moored upward-looking sonar on the Mackenzie shelf provides further insight into the ice growth and deformation regime governing sediment entrainment. Analysis of Radarsat Synthetic Aperture (SAR) imagery in conjunction with bathymetric data help constrain the water depth of sediment resuspension and subsequent ice entrainment (>20 m for the Chukchi Sea). Sediment loads averaged at 128 t km^{-2}, with sediment occurring in layers of roughly 0.5 m thickness, mostly in the lower ice layers. The total amount of sediment transported by sea ice (mostly out of the narrow zone between the landfast ice edge and waters too deep for resuspension and entrainment) is at minimum 4×10^6 t in the sampling area and is estimated at $5–8 \times 10^6$ t over the entire Chukchi and Beaufort shelves in 2001/02, representing a significant term in the sediment budget of the western Arctic Ocean. Recent changes in the Chukchi and Beaufort Sea ice regimes (reduced summer minimum ice extent, ice thinning, reduction in multi-year ice extent, altered drift paths and mid-winter landfast ice break-out events) have likely resulted in an increase of sediment-laden ice in the area. Apart from contributing substantially to along- and across-shelf particulate flow, an increase in the amount of dirty ice significantly impacts (sub-)ice algal production and may enhance the dispersal of pollutants.

Keywords: Sea ice; Ice rafting; Ice drift; Coastal processes; Shelf sedimentation; Arctic

*Corresponding author. Fax: +1 907 474 7290.
E-mail addresses: hajo.eicken@gi.alaska.edu (H. Eicken), gradinger@ims.uaf.edu (R. Gradinger), nunatech@usa.net (A. Gaylord), mahoney@gi.alaska.edu (A. Mahoney), igr@apl.washington.edu (I. Rigor), mellingh@dfo-mpo.gc.ca (H. Melling).

0967-0645/$ - see front matter © 2005 Elsevier Ltd. All rights reserved.
doi:10.1016/j.dsr2.2005.10.006

1. Introduction

Research over the past two decades has established that sediment-laden or "dirty" sea ice is a common phenomenon in the Arctic Ocean and its marginal seas. While the entrainment of sediments into newly grown sea ice had been reported in early, mostly anecdotal reports (see discussion in Pfirman et al., 1990), more recent icebreaker expeditions (Larssen et al., 1987; Pfirman et al., 1989; Reimnitz et al., 1993a; Nürnberg et al., 1994; Eicken et al., 2000; Tucker et al., 1999) and shore-based research (Osterkamp and Gosink, 1984; Kempema et al., 1989; Dethleff et al., 1993; Macdonald et al., 1995; Stierle and Eicken, 2002) have demonstrated that sediment-laden ice appears to be a common phenomenon. At the same time, detailed analysis of sediment cores obtained throughout the Arctic revealed that sediment transport by sea ice has been dominating the sedimentation regime in the Arctic Ocean and the Greenland Sea in the recent geological past (Clark and Hanson, 1983; Bischof and Darby, 1997; Nørgaard-Pedersen et al., 1998; Behrends, 1999). Apart from transferring organic carbon (including high fractions of terrigenous carbon, Eicken, 2003), sea-ice transport of sediments plays an important role in the redistribution and dispersal of pollutants (Lange and Pfirman, 1998) and is of importance for sea-ice microbial communities (Junge et al., 2004). Due to the sensitivity of ice optical properties to even small concentrations of opaque impurities the entrainment of sediments impacts the surface energy balance of the ice cover and significantly reduces the fluxes of short-wave radiation into the underlying water (Warren, 1984; Light et al., 1998; Frey et al., 2001).

The details of the entrainment process are still not well understood, although field work (Osterkamp and Gosink, 1984; Kempema et al., 1989; Reimnitz et al., 1993b; Stierle and Eicken, 2002), lab experiments (Reimnitz et al., 1993c; Ackermann et al., 1994; Lindemann, 1999; Smedsrud, 2001), and modeling (Sherwood, 2000; Smedsrud, 2002) have resulted in some progress in the recent past. From this work, it appears that sediment entrainment into sea ice requires resuspension of sediments during episodes of frazil ice formation. Work by Kempema et al. (1989) also suggests that the interaction between frazil crystals and the seafloor may promote resuspension of particulates. The degree of interaction between frazil ice and resuspended sediment particles depends on a number of parameters (grain size, wave height, water depth, current speed, initial stratification), but generally sediment entrainment is limited to water depths shallower than 30 m and is most effective in water depths less than 20 m (Reimnitz et al., 1987; Kempema et al., 1989; Sherwood, 2000). The potential role of anchor ice formation in dislodging sediments from the seafloor (Reimnitz et al., 1987) as well as the filtration of turbid water by ice slush at the surface (Ackermann et al., 1994) are not well understood but are assumed to be of lesser quantitative importance.

The broad, shallow Siberian shelves with fall ice formation over vast stretches of the seasonally ice-free marginal seas provide ideal conditions for the entrainment and export of sediments (Reimnitz et al., 1994; Eicken et al., 2000). Field observations (Lindemann, 1999; Dethleff et al., 1993, 2000), remote sensing (Eicken et al., 2000; Huck et al., submitted), analysis of sea-ice trajectories and modeling (Pfirman et al., 1997) as well as deep-sea sediment cores (Nørgaard-Pedersen et al., 1998; Behrends, 1999) underscore the importance of ice transport of sediments from the Siberian shelves. In contrast, the Chukchi and Beaufort shelves (Fig. 1), with comparatively narrow width and deeper waters, the lack of an extensional sea-ice drift regime, and—until very recently—a predominance of perennial ice, appear to be less important as source areas of sediment-laden sea ice (Reimnitz et al., 1993a, 1994; Eicken, 2003). Nevertheless, based on an analysis of ice-transported mineral grains, Darby (2003) concluded that the Banks Island shelf in the eastern Beaufort Sea represents an important source area. A recent study of the carbon and sediment budget of the Mackenzie shelf established that the role of sea-ice transport of organic carbon and particulates is a major unknown, with more data and insight required for closure of the budget (Macdonald et al., 1998).

With the exception of a pioneering study by Reimnitz et al. (1993b) comprising field work and remote sensing, little work other than studies of processes at individual localities (Barnes et al., 1982; Osterkamp and Gosink, 1984; Kempema et al., 1989) has been completed on sediment transport by sea ice in this region of the western Arctic. In contrast, a larger number of icebreaker expeditions (Larssen et al., 1987; Pfirman et al., 1989; Nürnberg et al., 1994; Eicken et al., 1997, 2000), land-based or airborne studies (Dethleff et al., 1993), and remote

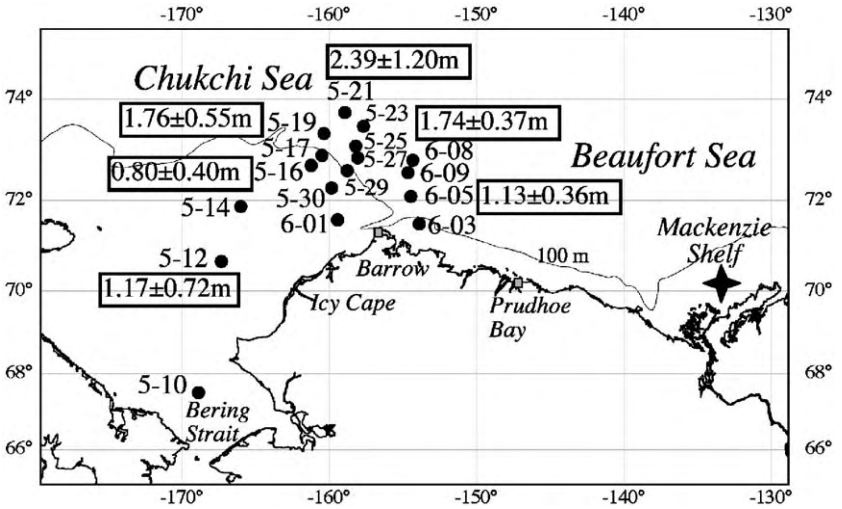

Fig. 1. Study area and ice-core sampling sites along USCGC Healy cruise track in May/June 2002 (core numbers indicate month and day of sampling). The numbers in boxes next to selected sampling locations indicate the mean and standard deviation of ice thickness as determined along profiles covering the sampling sites. The large asterisk denotes the location of upward-looking sonar mooring site. The 100-m isobath is shown in lighter gray.

sensing (Eicken et al., 2000; Huck et al., submitted) have focussed on the Eurasian Arctic seas. Here, we report on observations of sediment-laden ice in the Chukchi and western Beaufort Sea made during a late-spring icebreaker cruise in 2002. Ship-based observations are combined with analysis of sea-ice cores and remote-sensing data to arrive at an assessment of the amount of sediment entrained and exported, its origins and entrainment conditions as well as the importance of ice-transport of sediments in the context of shelf–basin interactions in this region of the Arctic Ocean. One of the unexpected findings of this study was the ubiquity and high concentration of sediments in particular in the lower layers of sea ice. This raises the question as to whether sediment export from this region by sea ice has been underestimated due to a lack of suitable observational efforts, or whether changes in the large-scale sea ice and surface circulation regime (Tucker et al., 2001; Comiso, 2002; Rigor et al., 2002) are responsible for increased entrainment and export. The question is addressed below.

2. Methods

2.1. Ship-based observations

The study area was traversed by the US Coast Guard Icebreaker "Healy" in May and June 2002 (Fig. 1). While the ship was underway, standardized ice observations were carried out from the ship's bridge at two-hour intervals for 10 min and once at every sampling site (Figs. 1 and 2) by a team of four observers. Observations covered a corridor of 1 km width to either side of the ship's track and comprised determination of prevailing ice types, ice thickness, snow depth, distribution of open water as well as estimates of ice affected by colonization by ice algae ("brown ice") and the areal fraction, small-scale distribution, and degree of sediment loading of "dirty" ice, visibly discolored by sediments. The degree of loading was estimated visually (high—ice layers of dark chocolate color; medium—patches of dark colored ice with lower concentrations and clean patches interspersed; low—few, small dark patches with faint sediment loading predominant). These semi-quantitative, visual estimates of areal fractions are associated with a significant error for areal fractions between about 0 and 90%, when we estimate a relative error on the order of 30%. For higher areal fractions of a given ice type or sediment-loading, the error is estimated as $<10\%$. Digital photographs of ice conditions to port and starboard and photographs of ice features were used to calibrate observations. A total of 182 observations was completed, and data and photographs are available on-line through the JOSS SBI Data Catalog (www.joss.ucar.edu/sbi/catalog). In addition, photographs of stratigraphic cross-sections of the ice cover were obtained by

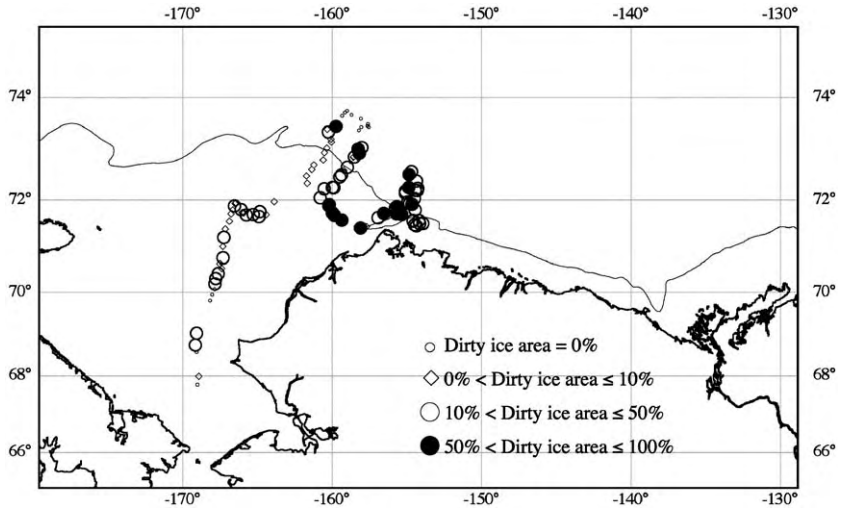

Fig. 2. Distribution of sediment-laden ice based on observations along the USCGC Healy cruise track. Symbols indicate the area occupied by sediment-laden ice (none, $\leqslant 10\%$, $\leqslant 50\%$, $\leqslant 100\%$).

taking images of ice floes broken and rotated 90° on their side along the ship's hull, which was a regular occurrence during standard icebreaking in level ice.

2.2. Sea-ice sampling and measurements

On 17 ice floes, snow samples and ice cores were obtained for measurements of snow and ice properties (Fig. 1). Sampling sites were chosen in ice deemed representative of the area based on surface morphology. Sediment concentration was not a criterion (and was difficult to estimate other than in broken ice). Immediately after drilling with a 9-cm diameter, fiberglass barrel, CRREL-type corer, photographs of ice stratigraphy along the entire core were obtained. Ice temperature was determined with a thermistor probe after drilling small holes into the core at the site. The core was then cut into 5–10-cm segments and placed in containers for melting aboard ship. At selected depth intervals, 10-cm vertical thick sections were cut and transferred frozen to the Geophysical Institute cold laboratory for production of thin sections for ice textural analysis (as described in Stierle and Eicken, 2002). On the vessel, ice salinity was measured with a YSI 85 conductivity probe (measurement error <0.02 or $<1\%$ of the bulk salinity, whichever is larger) and sub-samples transferred to 30-ml glass vials for measurements of stable-isotope composition at the stable-isotope facility at the International Arctic Research Center, University of Alaska Fairbanks. Samples were equilibrated against CO_2 for 12 h at 18 °C with subsequent measurement in a Finnigan MAT-252 mass spectrometer. Internal standards of South Pacific water and Fairbanks precipitation were calibrated against Vienna Standard Mean Ocean Water (VSMOW) and Standard Light Antarctic Precipitation (SLAP), with standard deviations $<0.05‰$. The remainder of selected ice samples was filtered onto pre-combusted, pre-weighed GF/F Whatman filters and washed with deionized water. The sediment concentration (suspended particulate matter, SPM) was calculated from the dry weight of particulates on the filter. At selected sites, smear slides were prepared of sediment samples and examined under a polarizing microscope to determine grain size, shape and mineral composition.

Ice thickness and snow depth were determined along 19 profiles on 15 floes (>8 km of total profile length at 5 m spacing). Measurements were carried out with an electromagnetic induction device (Geonics EM-31), and conductivity data have been inverted based on electromagnetic modeling and empirical relations derived by Haas and Eicken (2001) and Eicken et al. (2001). Additional direct measurements were carried out for validation purposes during the cruise. For comparison, ice growth and melt was also monitored at sea-ice mass balance sites near Barrow, with details provided by Perovich et al. (2001, see also www.arcticice.org).

2.3. Back-trajectory calculations

The potential source area of sediment-laden ice was estimated based on drifting buoy trajectories

made available through the International Arctic Ocean Buoy Program (IABP, web site at http://iabp.apl.washington.edu). An array of five principal buoys had been released in the eastern and central Beaufort Sea in October of 2001 as part of an ice-mechanics project (Richter-Menge et al., 2002a), and the likely trajectories of ice from several sampling sites were derived from back trajectory analysis using the gridded fields of ice motion described by Rigor et al. (2002). In addition, ice velocities and hypothetical trajectories were obtained from Doppler sonar ice velocity observations at a mooring site over the Mackenzie shelf (Melling et al., 1995; Galloway and Melling, 1997).

2.4. Analysis of bathymetry and remote-sensing data

The distribution of different ice types, open water, and the location of the landfast ice edge were determined through analysis of Radarsat Synthetic Aperture Radar (SAR) data and Advanced Very High-Resolution Radiometer (AVHRR) data covering the study area. A mosaic of C-band (5.3 GHz), ScanSAR wide scenes (100 m pixel size) covering the entire shelf between approximately 130 and 160°W was produced for each month from October 2001 to June 2002. Programs provided by the Alaska Satellite Facility (ASF) were employed for processing of SAR data, including calibration and geolocation. Based on temporal changes evident in monthly mosaics and drawing on additional AVHRR scenes and ground truth data, the landfast ice edge was delineated manually in all scenes. For periods of reduced cloud cover, AVHRR visible and infrared channel scenes (1.1 km pixel size, with resolution degrading away from the sub-satellite point) were obtained from the National Oceanic and Atmospheric Administration (NOAA) Satellite Active Archive for a total of 38 days during the observation period. Scenes were manually navigated based on ground control points and the coastline using a software package (Terascan) to minimize geolocation errors.

The National Ocean Service's (NOS) 10-m Coastal Bathymetry of the Bering, Chukchi, and Beaufort Seas was analyzed for the US portion of the study region. Over 300,000 depth soundings were acquired from various sources to create a 5-m bathymetry data set covering the nearshore area between Wainwright/Icy Cape east to the Mackenzie Bay, Canada. For Alaska, the GEODAS (GEOphysical DAta System) depth soundings acquired from the National Geophysical Data Center (NGDC) were the primary data source. This information was supplemented with depth soundings derived from the NOAA Electronic Nautical Chart for the Beaufort Sea and the United States Minerals Management Service (Outer Continental Shelf Study MMS 2002-017). In addition, depth soundings in feet below mean lower low water (MLLW) were digitized from the July 28, 1990 (1:47943 scale) NOAA #16082 nautical chart for Point Barrow. The Canadian sounding data extending to the Mackenzie Delta were derived from the Digital Ocean™ product created by Nautical Data International for the Canadian Hydrographic Service (Mackenzie Bay Chart 7662 and Demarcation Bay To Philips Bay Chart 7661, Copyright © Her Majesty the Queen in Right of Canada—Canadian Hydrographic Service). The sounding data were used to generate a gridded data set from which contours were derived using a kriging technique with Geographic Information Systems (GIS) software from the Environmental Systems Research Institute. The water depth along the landfast ice margin was determined by intersecting the bathymetry polygons with 250-m grid cells representing the landfast ice edge as determined from the SAR scenes.

2.5. Weather data and ice-growth modeling

A simple freezing-degree day ice-growth model was employed to estimate the approximate age of different ice types sampled in the field. The model derives the ice thickness H at time t according to

$$H^2 + (13.1\,h + 16.8)\,H = 12.9\,\theta$$

with h the mean snow depth and θ the number of freezing-degree days. The model has been validated with mass-balance data collected at Barrow (details provided in Eicken, 2003).

Weather data (wind speed, direction, and air temperature) measured at hourly intervals were obtained from National Weather Service stations at Barrow and Prudhoe Bay (Deadhorse).

3. Results

3.1. Regional distribution and stratigraphic cross-sections of sediment-laden sea ice

The distribution of sediment-laden ice as determined from ship-board observations and ice coring

is shown in Fig. 2. Of 183 observations, 61% revealed sediment-laden ice, with an average areal sediment-laden ice fraction of 19%. During the first half of the cruise snow cover concealed surface features. Also, sediments were frequently confined to the lower layers of the ice. Hence, the areal fractions of sediment-laden ice are minimum estimates. Ice coring and visual observations after complete removal of the snow cover during the last days of the cruise in mid-June indicate that sediment areal fractions may have been underestimated by as much as a factor of two. Most sightings were of medium sediment-laden sea ice (33% of all observations), while high and low sediment concentrations accounted for 12% and 16% of all observations, respectively. The highest areal fraction of sea ice containing sediments and the highest sediment concentrations were observed along the two SSW–NNE transects in the eastern half of the study area, with 29% of the total ice area consisting of sediment-laden ice. The northernmost stretches of cruise track (north of 73°N, Fig. 2) extended into the multi-year ice pack as detailed in Section 3.2 below. This ice looked clean and ice-core samples were likewise free of lithogenic particulates other than the background concentration of marine detritus (concentrations of a few $mg\,l^{-1}$, Reimnitz et al., 1993a; Eicken et al., 1997). The southern Chukchi Sea was also comparatively free of sediment-laden ice.

Systematic observations of cross-sections of ice floes broken and turned over by the ship revealed the following sediment distribution and ice-stratigraphy patterns:

Type 1: Sediments distributed evenly throughout the upper layers of the ice cover (Fig. 3A, B). This type of ice, often referred to as turbid ice (Kempema et al., 1989), was comparatively rare in its pure form (Fig. 3A) and was observed mostly in the western and central parts of the study area.

Type 2: Thicker layers of finely dispersed sediments but with layering evident from ice growth and deformation events (Fig. 3C, D). This type of ice along with type (3) was most common and occurred in particular in the eastern and central section of the study area. Fig. 3D shows a representative example with stacks of sediment-laden ice that accumulated under cleaner ice of comparable single-layer thickness.

Type 3: Rafted (defined here as the result of the process of subparallel stacking of level pieces of ice) and fragmented layers of clean ice with sediment dispersed throughout a solidified frazil and brash ice matrix filling voids between original rafts and fragments (Fig. 3E, F). This type was quite common, with ample evidence of substantial fragmentation and deformation of the sediment-free ice cover. Fig. 3F represents a transition to type (4) but is typical of a large number of observations with sediment confined to the lower layers of the ice cover.

Type 4: Well-defined layers of high sediment concentrations within a turbid or frazil ice matrix (Fig. 3G). This type of ice was also quite common throughout the central and eastern study area. Typically, sediment layers were found at the base of turbid or frazil ice, overlying or delineating the contours of rafted or fragmented pieces of ice. The lateral extent of these layers varied from a few decimeters (Fig. 3F) to several meters or even tens of meters (Fig. 3G).

Type 5: Surface sediment patches. Towards the end of the cruise, patches of cm-thick layers of sediments were observed on the ice surface (and at the bottom of meltwater layers) at a few locations. These features are interpreted as the result of surface melt with subsequent retention and concentration of sediments at the ice surface.

3.2. Properties of sediment-laden ice, sediment characteristics and particulate loadings

Both, ship observations and thickness profiling at ice sampling sites revealed a distinct trend of increasing ice thickness towards the northern part of the study area. The northernmost locations (Figs. 1 and 2) were located in multi-year sea ice (>95% of total area). Multi-year ice was identified based on its thickness (modal winter ice thickness of level ice >1.8 m, Perovich et al., 2003), rolling surface topography and the characteristic salinity profile with salinities <0.5‰ throughout the uppermost decimeters of the ice cover, increasing gradually to values of >3‰ in the lower half of the ice (Untersteiner, 1968; Eicken et al., 2002). First-year ice, on the other hand, was completely smooth and level in undeformed areas, exhibited modal winter ice thicknesses of level ice below 1.7 m, and apart from a small reduction in salinity to values of around 1‰ in the uppermost 10–20 cm as a result of early melt in June of 2002 did not show any reduction in ice salinity due to meltwater flushing, with values of 4–5‰ or higher. The youngest ice, as estimated from the thickness of level ice, was found

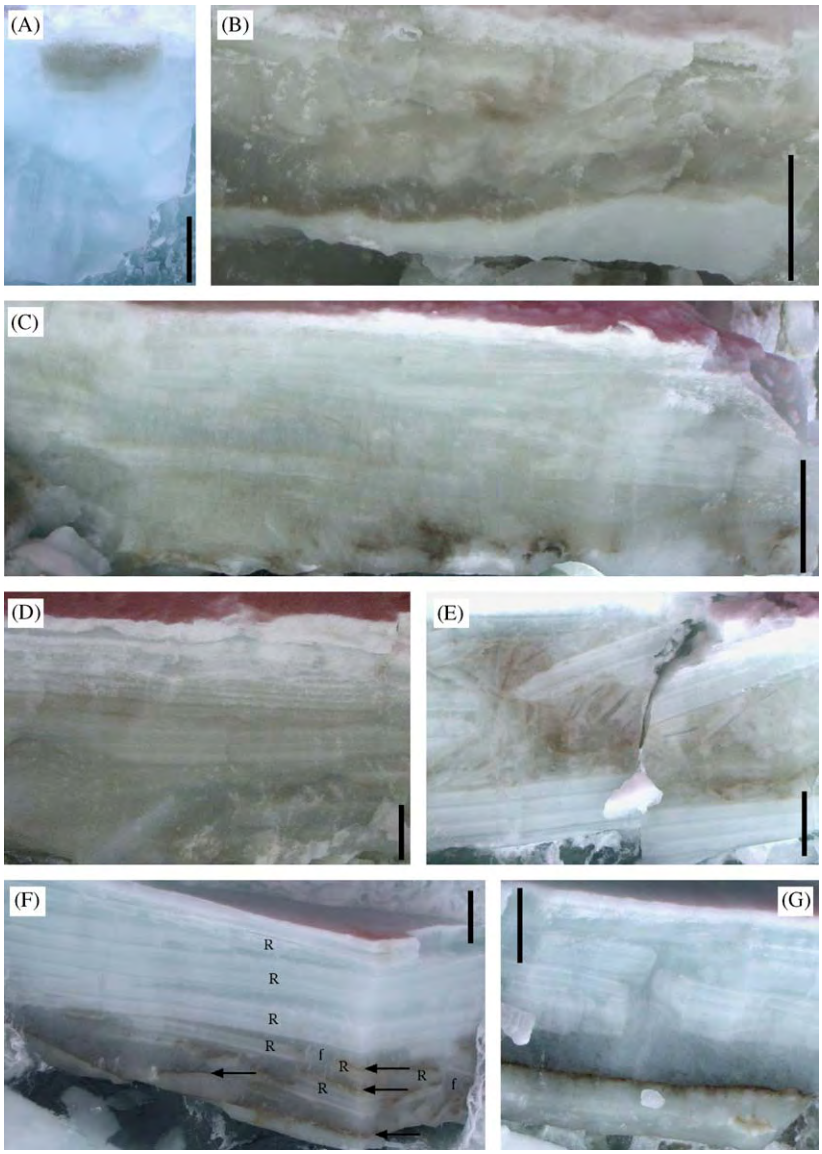

Fig. 3. Stratigraphic cross-sections and sediment distribution within ice floes broken and turned over on their side along the ship's hull. All photographs have been aligned so as to show the ice stratigraphy in proper orientation with the top of the floe up. The scale bar on each image is 0.5 m. (A) Block of turbid ice within fine-grained surface ice layer, May 26. (B) Turbid ice layer with interspersed blocks of sediment-laden brash ice, June 10. (C) Ice floe with higher concentrations of sediments in the form of turbid ice and as sediment-rich patches in the lower layers of the ice, June 11. (D) Rafted and deformed layers of sediment-laden ice, June 5. (E) Rafted and fragmented layers of clean ice with sediment dispersed throughout solidified frazil and brash ice matrix, June 7. (F) Layers of sediments among turbid ice matrix interspersed with and underlying multiple rafts of clean ice, June 7; some of the sediment layers have been marked by an arrow, "R" indicates individual ice rafts and "f" shows some of the frazil ice matrix enveloping ice fragments. (G) Sediment-rich layer at base of frazil ice layer, overlying clean ice raft, June 7. For approximate locations see Fig. 1 with same-day sampling locations.

in the southern Chukchi Sea (site 5–10, level-ice thickness 0.57 ± 0.06 m, and site 5–12, level-ice thickness 0.92 ± 0.08 m). While the ice was generally thicker in the western Beaufort Sea, stratigraphic studies revealed that this was mostly due to dynamic thickening (rafting and ridging) of thinner ice sheets (Fig. 3D, F) and frazil ice accumulation (Fig. 3A, B, Fig. 4) rather than undisturbed ice growth. The thickness of the parent ice sheets involved in the rafting and ridging process as determined from

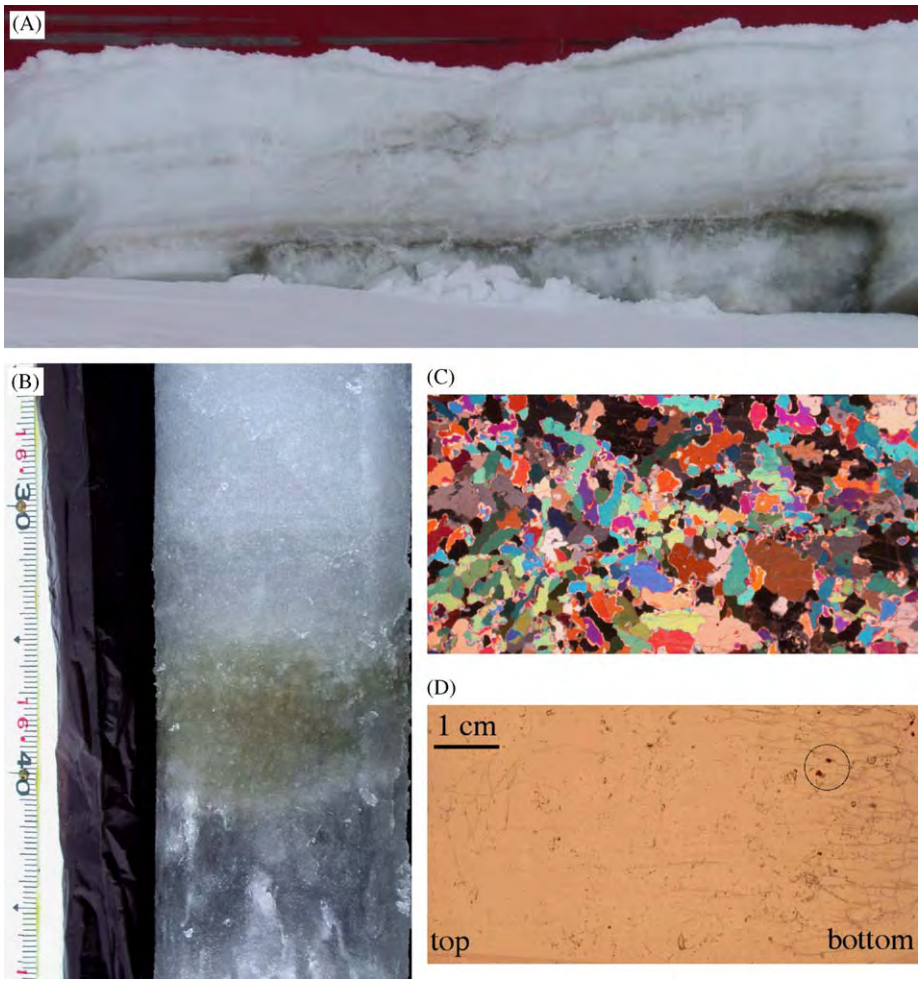

Fig. 4. Sediment inclusions within sea ice observed at different scales. (A) Cross-section of ice floe (approximately 1 m thick) rafted onto ice sheet by ship at site 5–12. Note the dark layers of sediment in the interior and at the bottom of the ice cover, including a zone surrounding an entrained fragment of ice. (B) Core photograph between 0.35 and 0.47 m depth at site 5–12 (scale shown at left). Note the band of sediment inclusions at the base of a granular ice layer (milky appearance) derived from frazil ice, with clearer columnar ice below sediment band. (C, D) Thin-section microphotographs of a granular ice layer (core 5–12, top is to the left) containing sediment inclusions photographed between crossed polarizers (C) and in plain transmitted light (D). Two sediment aggregates of 1–2 mm diameter are highlighted by a circle in (D).

ice observations (Fig. 3D–G) varied between 0.1 and 0.4 m. Ice floes visibly deformed by ridging, rafting or through the formation of rubble and brash ice accounted for a very high fraction of the total ice area (18% based on ice observations) and the ice stratigraphy indicates that even the level ice contained a significant fraction of deformed ice.

Core stratigraphic and microstructural analysis (Fig. 4) revealed that sediment inclusions were invariably associated with granular ice resulting from consolidation of frazil ice crystals accumulating at the ocean surface (as in Fig. 3A or 4A) or the base of the ice sheet (as in Fig. 3F or 3G, with fragments of the broken up parent ice sheet enveloped in a frazil matrix). Sediment inclusions were found throughout the entire ice thickness (summary data shown in Table 1). The total sediment loading per unit area parallels the ship-based observations of sediment areal extent and degree of ice discoloration (Fig. 2), with the southwesternmost sample from thin ice exhibiting the lowest value and highest loadings observed along the easternmost transects.

At site 5–16, characterized by moderate to light sediment loading based on ice observations and examination of cores drilled at the site, smear slide

Table 1
Concentration and loadings of sediment-laden ice

Site	Ice thickness (m)	Sediment layer thickness (m)	Sediment layer salinity (‰)	SPM ($mg\,l^{-1}$)	n	Sediment loading ($g\,m^{-2}$)
5–12	0.9	0.15	5.5	463	2	69
6–01	3.9	0.91	2.4	91	3	83
6–05	2.02	0.40	3.4	508	6	203
6–08	2.05	0.51	4.1	306	1	157

SPM—Mean concentration of suspended particulate matter, n—number of cores taken at each site.

analysis showed the sample to be dominated by fine silt and clay (mostly lithogenic material with few diatom frustules and other biogenic particles) with typical grain sizes of a few micrometers and maximum grain sizes of around 20 μm. Ice-transported sediments at site 5–30, with significantly higher sediment concentrations and areal extent, consisted mostly of fine sand and coarse silt (high fraction of quartz, with some aggregates of fine grained minerals and few biogenic particles), with typical grain and aggregate sizes of 100 μm and maximum grain size around 250 μm.

The stable oxygen isotope composition ($\delta\,^{18}O$) of three sediment-laden ice cores from the western, central and eastern part of the study area is shown in Fig. 5. The lowest $\delta\,^{18}O$ were found in the East (core 6-05) with a mean value of -1.9 ± 0.9 ‰, with core 5–16 exhibiting the highest $\delta\,^{18}O$ of 0.6 ± 0.6‰ and the westernmost core (5–12) averaging at -1.5 ± 1.8‰. With the exception of a single layer in core 5–12 (part of a rafted piece of ice, possibly contaminated by snow) $\delta\,^{18}O$ increased with depth and there was no distinct correlation between sediment concentration and isotopic composition as evident from Fig. 5.

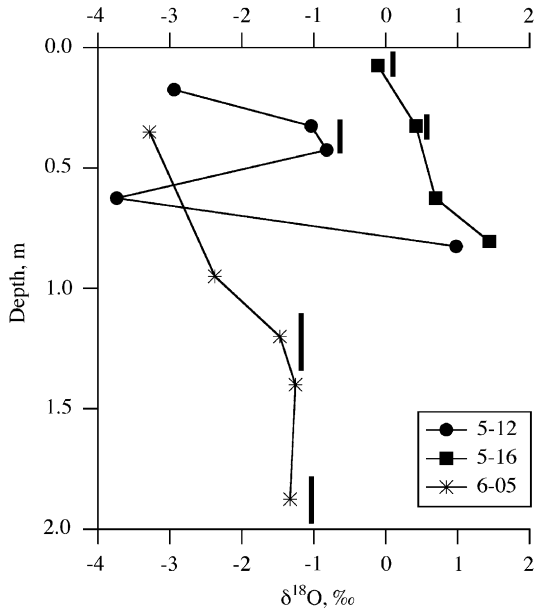

Fig. 5. Stable isotope composition ($\delta^{18}O$) of ice cores from western, central and eastern part of study area (see Fig. 1 for locations). Black bars denote the extent of sediment-laden ice in core.

3.3. Backtracking the origins of sediment-laden ice

The reconstructed sea-ice trajectories indicate two different potential source areas for the ice in the southeastern Chukchi and western Beaufort Sea (Fig. 6). For the former, trajectories originate from along the coast between Icy Cape and Barrow, with an estimated ice age of 1–3 months. The age is likely underestimated, since the optimal interpolation scheme for deriving ice velocity fields does not account for ice-coast interaction, which has a tendency to slow down the ice as compared to interpolated trajectories. Ice also may have been transported to the trajectory origin from farther east along the coast, as indicated by the predominantly westward drift of buoy 22206, followed by swift veering of ice motion in conjunction with changes in the wind field (Fig. 7).

Trajectories for the ice sampled in the North and East of the study area follow the general outline of the coast and trail off into the area north of the Canadian Archipelago (Fig. 6). This indicates an origin of the ice in the Beaufort Sea, but owing to the limitations of the trajectory backtracking method does not allow conclusions about the exact source area(s) between Barrow and the Mackenzie Delta. Based on the ice thickness measurements, ice texture and salinity profiles, we can eliminate any possibility of the ice having formed prior to the previous fall freeze-up. This would place the simulated trajectories in deeper water off the Mackenzie shelf during freeze-up. The trajectory

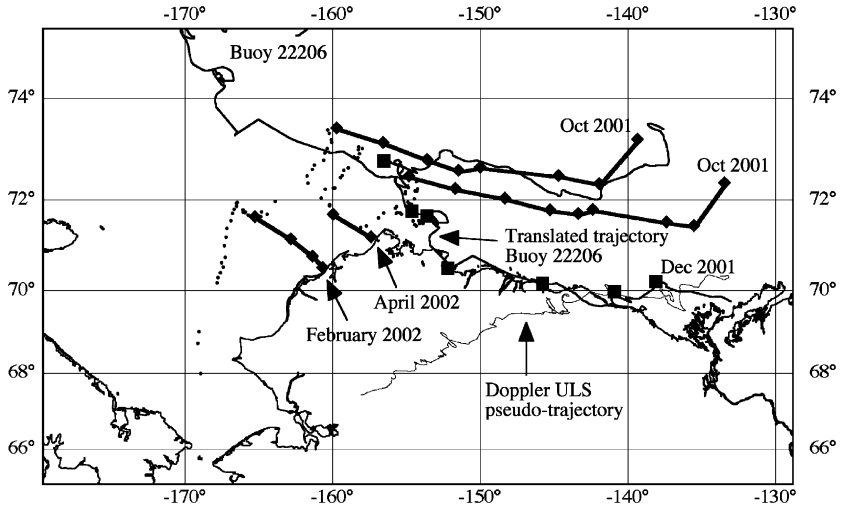

Fig. 6. Simulated and observed ice trajectories in the study region. Shown are the original trajectory of Buoy 22206 and the translated trajectory of the buoy, extrapolated to the sediment-laden ice area (solid squares indicate position of buoy during previous months). The thick solid lines show the simulated ice trajectories for four sampling sites (solid diamonds indicate position of buoy during previous months). The thin line delineates the pseudo-trajectory derived from Doppler upward-looking sonar (ULS) measurements at a mooring site north of the Mackenzie Delta (trajectory originates at mooring location). Note that for all trajectories ice motion is from east/right to west/left.

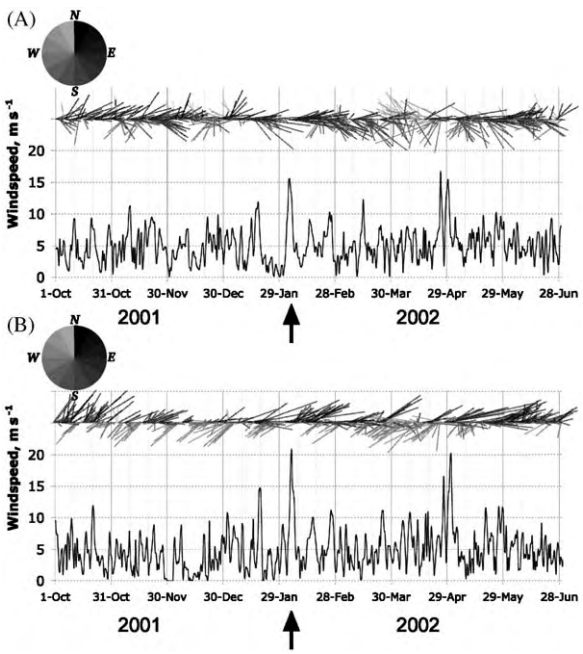

Fig. 7. Wind velocity (12 h averages) measured at the National Weather Service Stations in (A) Barrow and (B) Prudhoe Bay (Deadhorse) for the time period from October 1, 2001 to June 1, 2002. The wind velocity vectors (pointing upwind) are shown at the top of each panel, with the speed plotted below. The arrow denotes the storm event from February 3–5 discussed in more detail in the text and shown in Fig. 8.

of buoy 22206, which passed through the study area and was roughly 500 km to the Northwest at the time of sampling (Fig. 6), also supports an origin between the central Beaufort Sea and the Mackenzie shelf between October and March (Fig. 6).

An upward-looking Doppler Sonar mounted on a mooring north of the Mackenzie Delta provided further ice-velocity data that more accurately reflect the complex motion resulting from ice-coast interaction. A hypothetical trajectory derived for an ice parcel forming at freeze-up at the mooring site (Fig. 6) indicates that (1) north of the Mackenzie Delta, ice motion was mostly directed toward WSW, with the potential for significant export of newly formed ice from a flaw lead or coastal polynya over the northeastern Mackenzie shelf where the landfast ice edge trends roughly SSW–NNE, and (2) even the reduced ice velocity in the shallower shelf waters, with episodes of stagnant ice in late October, December/January and April, was sufficiently high to transport sea ice from the Mackenzie shelf into the eastern half of the study area.

3.4. Remote-sensing and weather data from potential source areas of sediment-laden ice

Over the eastern Beaufort shelf freeze-up commenced around October 10 and was mostly complete

by October 25, 2001, whereas the western half of the Beaufort shelf experienced freeze-up between October 1 and 15 based on examination of passive microwave satellite data (NSIDC, 2002). Direct observations of freeze-up in Elson Lagoon near Barrow (October 2) and the coastal waters around Barrow (October 12) corroborate these findings.

Wind velocities at Barrow and Prudhoe Bay from just prior to freeze-up to the start of the sampling campaign are shown in Fig. 7. Conditions during freeze-up at Barrow were calm, with a mean wind speed of 4.6 m s^{-1} (October 1–15). Except for a one-day storm with a maximum wind speed of 10.3 m s^{-1}, values did not exceed 8 m s^{-1}. Our own field observations and analysis of ice cores obtained along the coast from landfast ice near Barrow indicate that these conditions did not result in much frazil ice formation or significant sediment entrainment. A late spring storm on April 30, 2002 is of little relevance for this study, as it occurred too close to the onset of melt to have resulted in significant ice formation. However, a major storm from February 3 to 5, with peak wind velocities of 18 and 25 m s^{-1} (out of ESE) at Barrow and Prudhoe Bay, respectively, was important. Examination of AVHRR satellite imagery from November to April, indicates that of all the periods with hourly wind velocities higher than 10 m s^{-1}, this event generated the largest coastal polynya observed between Point Barrow and Icy Cape (Fig. 8) during the entire winter. Open water and thin ice were present for about a week, with subsequent closure through ice growth and shoreward movement of the ice pack (Fig. 8C). In the Beaufort Sea, the storm did not create much open water but resulted in ice deformation with a significant reduction in floe size (Fig. 8B).

The satellite scenes (AVHRR and Radarsat SAR) also demonstrated that with prevailing shore-parallel winds in the Beaufort Sea (Fig. 7B) and a tightly packed offshore ice pack filling the eastern Beaufort Sea and the Canadian Basin, few openings along the landfast ice occurred during the winter. In fact, it was not uncommon to observe complete stoppage of the ice pack southeast of a line connecting Point Barrow and the northern shores of Banks to Ellesmere Islands, as noted previously (Stringer, 1978). The SW–NE-trending lead visible in Fig. 8C marks this area of stagnant ice. The only episode of significant generation of open water along the western and central Beaufort Sea landfast ice edge occurred between February 27 and March 7, 2002 (Fig. 8D), and was associated with maximum windspeeds of 10 m s^{-1} from southwest (Fig. 7B). While the Doppler sonar mooring off the Mackenzie Delta registered an additional four

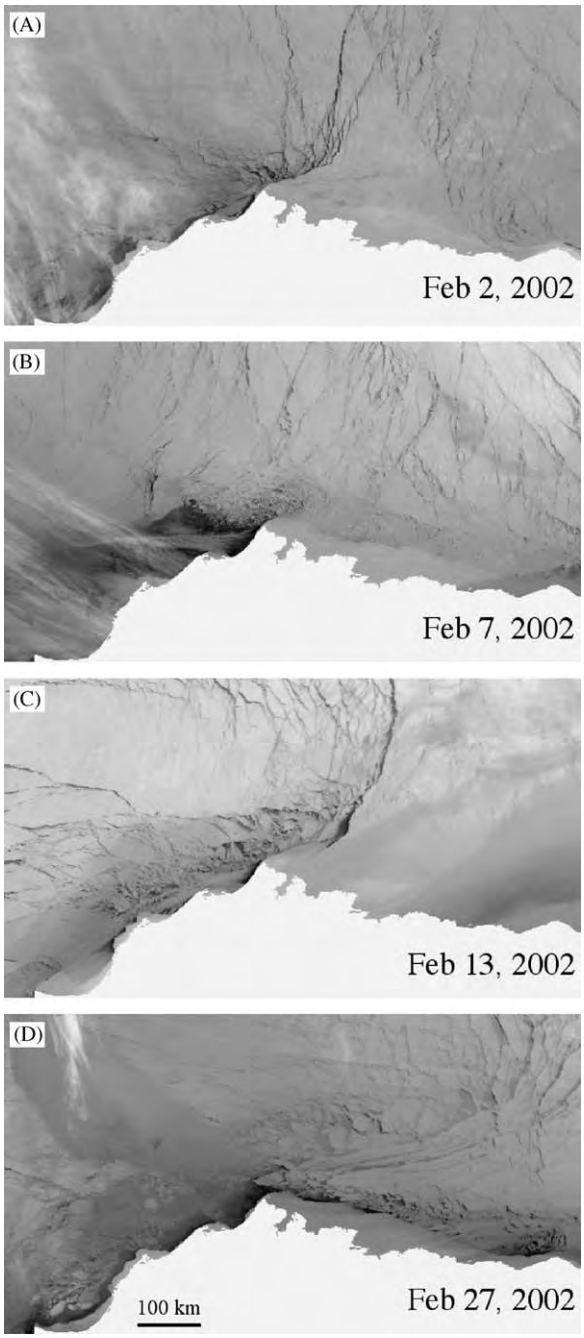

Fig. 8. AVHRR satellite scenes (channel 4, thermal infra-red) showing the study area before, during and after the major storm of February 3–5, 2002. Images have been derived from calibrated brightness temperature (T_B) scenes, with gray values inverted so as to show open water ($T_B \approx 271$ K) as black and colder ice in whiter shades. White streaks in western part of scenes are clouds.

significant opening events between November and February, the ice trajectories from these opening events fell short of reaching the study area (Fig. 6).

3.5. Bathymetry constraints on sediment entrainment

Field data and modeling indicate that sediment entrainment into sea ice is generally limited to water depths less than 30 m, and appears to be most effective in water shallower than about 20 m. Nevertheless, some modeling based on laboratory experiments (Smedsrud, 2003) suggests that given high sufficient wind speeds (18–25 m s^{-1}) and significant fetch, entrainment may be possible even in water as deep as 50 m. This is of lesser importance for the present study, however, since neither wind speeds nor fetch are sufficient for such conditions to develop (see also discussion below).

With the onset of landfast ice formation in October and November, much of the potential source area for sediment-laden ice is covered by fast ice that typically does not break free until well after the start of the melt season. Hence, mapping the location of the landfast ice edge in relation to bathymetry can provide substantial insights into the distribution of potential sediment entrainment areas during the course of winter. In late December 2001, 59% of the total length of the landfast ice edge in the Beaufort Sea was positioned at water depths between 0 and 15 m (Fig. 9). By early March 2002, the landfast ice had grown outward with 77% of the fast ice edge in waters between 0 and 25 m deep (Fig. 9). Maps showing the intersection of the landfast ice with the bathymetry (Fig. 10, Table 2), indicate that in mid-February most of the shallow water (<20 m) exposed to drift ice and hence potentially mid-winter sediment export is confined

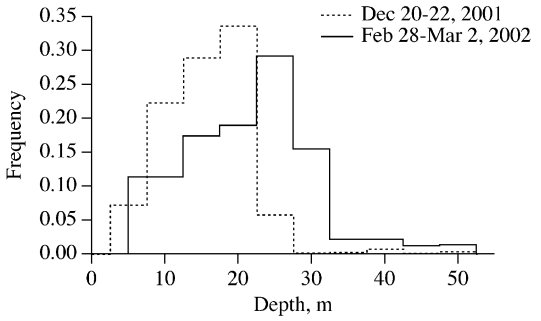

Fig. 9. Frequency histogram showing the water depth distribution at the landfast ice edge in the study area in early and mid-winter.

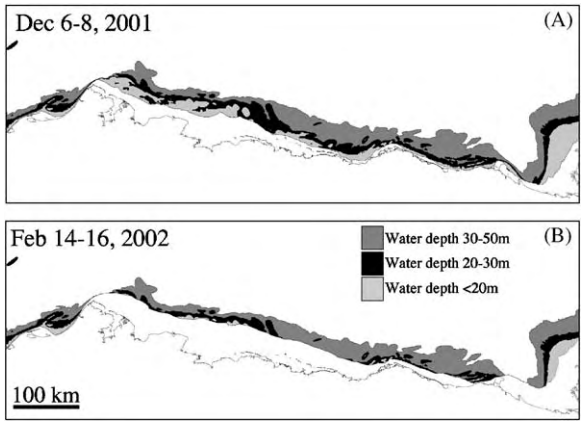

Fig. 10. Distribution of water shallower than 50 m outside of the landfast ice edge in the study area. Water depths between 50 and 30 m are shown in dark gray, between 20 and 30 m in black and water shallower than 20 m is shown in light gray. The landfast ice edge has been derived from Radarsat SAR scenes © for December 6–8, 2001 (A) and February 14–16, 2002 (B).

Table 2
Shallow water area outside of the landfast ice edge

Date	Water depth ⩽20 m (km^2)	Water depth >20 and ⩽30 m (km^2)	Water depth >30 and ⩽50 m (km^2)
December 6–8, 2001	9678	10,709	19,635
February 14–16, 2002	2617	6395	18,083

to an area in the easternmost Chukchi Sea between Point Franklin and Barrow, a few stretches of coastline, in the western and central Beaufort Sea, and a larger area off the Mackenzie Delta (Fig. 10B). It should be noted that Reimnitz et al. (1993b), based on microfossil finds in ice-transported sediments and indirect evidence, concluded that entrainment may occur down to depths of as much as 50 m. As evident from Fig. 10 and Table 2, the 50-m isobath is well outside of the landfast ice edge throughout almost the entire study area.

4. Discussion

4.1. Likely origins of sediment-laden ice and ice-growth history from ice stratigraphy and a simple model

The different types of ice drift data (Section 3.3, Fig. 6) indicate that the northeastern Chukchi coast

and adjacent shelf are the source of sediment-laden ice found in the southwestern part of the study area (see trajectories marked with February 2002 and April 2002 in Fig. 6). The young age of this ice is commensurate with growth in a coastal polynya environment in February/March (Fig. 8), which is also supported by weather records from the area (Fig. 7). Ice sampled to the North and Northeast of Barrow originated from along the Beaufort Sea shelf, some of it as far east as the western Mackenzie shelf (Fig. 6). Further constraints on ice origin and age can be obtained from the ice stratigraphy. A freezing-degree day model indicates that with a snow depth of 0.1 m (averaged over the course of the entire winter based on measurements at Barrow and during the sampling campaign), ice growth could at most account for an ice thickness of 1.71 m since freeze-up. Landfast ice formed in mid-October grew to a maximum thickness of 1.67 ± 0.10 m based on mass-balance measurements at Barrow. Sediment-laden ice averaged at 1.13 ± 0.36 m thickness in the southeastern stretches of the study area, with the thickness mode associated with level ice below 1 m, which based on the freezing degree-day model (and a snow depth of 0.05 m) suggests an age of 3.5 months and an origin west of Prudhoe Bay. Only in the northernmost first-year ice did we observe average thicknesses of between 1.7 and 1.8 m, with modal values for level ice well below 1.7 m. However, the ice stratigraphic analysis (Figs. 3 and 4) demonstrates that a significant fraction of this ice, and even the thinner ice to the South, was composed of multiple rafted layers with significant contributions of frazil ice to the total thickness, suggesting a younger age. The parent ice sheet of 0.1–0.4 m thickness formed in the month of February and subsequently deformed during rafting events (such as illustrated in Fig. 3E–G), is estimated as on the order of 3 days to 2 weeks old (based on the freezing-degree day model). While it is much more difficult to estimate the number and duration of individual rafting events (see, e.g., Toyota et al., 2004, for a more detailed discussion), the uniform thickness of ice layers such as those in Fig. 3F suggests that at least in some cases multiple stacking of ice rafts occurred in a single event.

Data obtained from the upward-looking sonar at the mooring site on the Mackenzie shelf (Fig. 1)

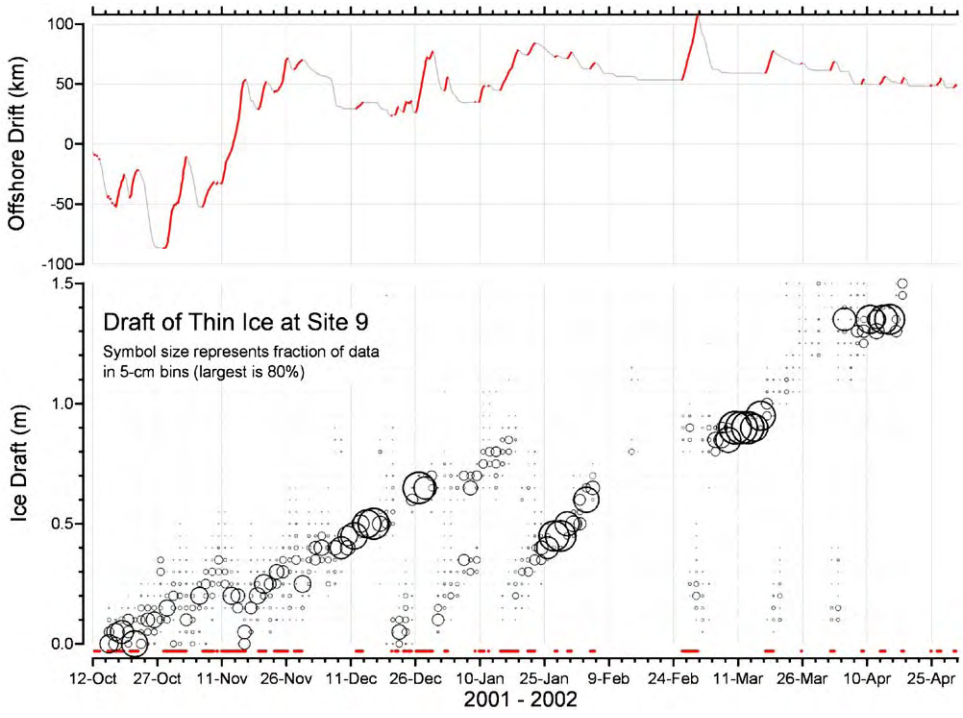

Fig. 11. Time series of ice draft (bottom) obtained from an upward-looking sonar moored on the Mackenzie shelf (Fig. 1). The size of the circles indicates the fraction of data in different ice thickness bins. In conjunction with the record of the offshore ice drift component (top) the data clearly show sequences of lead openings (denoted by thicker solid lines in top graph and time bars in the lower graph) and closings off the landfast ice edge.

confirm these events and provide further insight as illustrated in Fig. 11. The Doppler sonar identifies a number of episodes of lead opening with offshore ice drift, typically followed by onshore motion (e.g., December–January and February events in Fig. 11, top). The sonar confirms that these events resulted in significant new-ice production, as demonstrated by cohorts of shallow-draft ice that appear during the opening phase and then rapidly thicken during the closing phase. The latter appears to be greatly aided by rafting and ridging events, as thermodynamic growth alone is not able to explain thickening rates of this order of magnitude. The prevailing ice thickness classes (<0.1–0.4 m, Fig. 11) during these ice production episodes correspond well with the stratigraphic observations.

Ice stratigraphy and sediment distribution indicate that the entrainment process occurred after initial growth of an ice sheet 0.1–0.2 m thick, subjected to single or multiple rafting events. Entrainment of sediment was associated with formation of frazil ice, accumulating underneath the existing, rafted or ridged ice (Fig. 3E–G, Fig. 4). This type of ice growth appears similar to that characteristic of a coastal polynya environment where wind- or tide-induced open water lead to formation of nilas (composed of congelation ice without entrained sediments) or frazil, punctuated by episodic deformation events, as those evident in the ice draft/offshore ice-drift time series shown in Fig. 11. The striking stratigraphic sequences of clean nilas interlaced with sediment-laden frazil shown in Fig. 3 have not been reported in previous studies in the region (Reimnitz, pers. comm., 2004) and may require further explanation.

Typically, formation of frazil ice requires a minimum wind stress to generate sufficient wave action for frazil to form. An Antarctic coastal polynya study has indicated that the transition from nilas to frazil growth typically occurs at wind speeds around $10\,\mathrm{m\,s^{-1}}$ (Eicken and Lange, 1989). The stratigraphic sequence evident in cores and floe cross-sections and the mooring data shown in Fig. 11 suggest that it is the sequence of (1) polynya/lead opening, (2) formation of nilas (continuously exported during the offshore ice drift phase), (3) formation of frazil as wind speed and wave height increase, and (4) rafting and ridging with integration of the most recently formed frazil into a thickened ice sheet evident in stratigraphic cross-sections and ice draft data. Apart from the repeated opening and closing sequences and the nilas/frazil transition, such a scenario is similar to that proposed by Dethleff et al. (1993, 1998) for the flaw lead system of the Laptev Sea.

One question that this scenario (as well as any other mid-winter sediment entrainment) raises is to what an extent, or if at all, resuspension of sediments from the seafloor at water depths larger than 10 m (Figs. 9 and 10) can be explained by wave action in the flaw lead/polynya environment. The Mackenzie shelf moorings provide additional insight. Based on the measurements of significant wave height (up to a maximum of 1.7 m during the freeze-up phase on October 10, 2001; H. Melling, unpubl. data) orbital speeds can be derived for different water depths. Resuspension-threshold model predictions (Komar and Miller, 1973) indicate that even during the freeze-up period, when fetch and wave heights were highest, simple wave-driven resuspension only explains resuspension in water depths up to 15–20 m. As has been discussed previously (Kempema et al., 1989), this finding suggests that the presence of frazil ice in the water column is a prerequisite for sediment resuspension, and hence entrainment later in the season (assuming that currents are of insufficient magnitude to result in resuspension over these areas).

An origin in a well-mixed, nearshore environment late in the season is also supported by the oxygen isotopic composition of an ice sample north of Barrow (core 5-16, Fig. 5). Assuming a fractionation coefficient of 1.5–2‰ (Macdonald et al., 1995; Eicken, 1998), the water mass from which the ice formed has a $\delta\,^{18}$O lower by this amount, i.e. –1.4 to –0.9‰ for sample 5-16. Based on water-column stable isotope measurements during the 2002 USCGC Healy cruise (Cooper, unpubl. data; see also Cooper et al., 1997), this indicates an origin over the well-mixed inner shelf of the northeastern Chukchi or western Beaufort Sea. The lower values in particular of sample 6-05 indicate formation in an area with significant influx of river water. For sample 5–12 this could be the southern reaches of the Chukchi Sea, where river inflow reduces surface $\delta\,^{18}$O to below –3‰ (Cooper et al., 1997). For sample 6-05, a water mass of $\delta\,^{18}$O between –3.9 and –3.4‰ is commensurate with an origin over the western Mackenzie shelf, where winter surface water $\delta\,^{18}$O ranges between –2.5 and –5‰ (Melling and Moore, 1995; Macdonald et al., 1999). It should be noted, however, that neither the observed or interpolated buoy trajectories nor the ULS Doppler ice velocities indicate an origin

beyond the Mackenzie region, such as the Banks Island shelf.

4.2. Sediment transport by sea ice and potential relevance for shelf–basin interaction in the western Arctic

The total area of sediment-laden ice observed in spring of 2002 in the Chukchi and western Beaufort Sea amounts to roughly 110,000 km^2 (with the inner area of higher sediment load defined by a polygon between sites 5–12, 6–01, 6–03 and 5–23 covering 86,000 km^2, Fig. 1). The mean sediment load for this area as derived from ice core measurements amounts to 128 $g\,m^{-2}$ or t km^{-2} (Table 1). With an average sediment-laden areal fraction of 29% obtained from ice observations (Section 3.1), the total sediment load amounts to 4.1×10^6 t (or 4.1 Tg). Sediment loads increased towards the East and the easternmost sampling sites correspond to the furthest western extent of ice originating from the Mackenzie shelf, based on ice core data, drift records from buoys, a drift model and moored sonar ice-velocity measurements (Section 3.3, Fig. 6). Hence, it is likely that a significant sediment load was present in the ice of the central and eastern Beaufort Sea at the time of sampling, raising the total load of the eastern Chukchi and Beaufort Seas to between 5 and 8 Tg. Compared with previous observations (Kempema et al., 1989; Reimnitz et al., 1993b), this total area of sediment-laden ice is significantly larger.

Reimnitz et al. (1993b) described an "abnormally high" amount of sediment-laden ice formed in the central Beaufort Sea in January and February 1989 over the course of several weeks following a severe storm with peak wind velocities of 27 $m\,s^{-1}$. Despite the smaller area of sediment-laden ice surveyed in that study, the overall amount of sediment transported is likely to be of the same order of magnitude as the observations reported here, due to higher sediment loads (289 t km^{-2}). Some aspects of the 1989 entrainment event are comparable to the formation of sediment-laden ice in the eastern Chukchi Sea in February of 2002, including observations of sediment which "delineated a framework of individual ice blocks and slabs as much as 40 cm thick" (Reimnitz et al., 1993b; Fig. 3). The likely sediment entrainment areas appear to overlap to some extent as well. A major difference is the predominance of sediments in the lower ice layers in 2002, well concealed from surface observations other than those aided by icebreaking operations or exposure of sediments in ridged ice.

The amount of sediment transported in 2002 figures significantly in the sediment budget of the eastern Chukchi and western Beaufort shelves. Coastal retreat supplies at most 15,000 m^3 (approximately 20,000 t) of sediments per km of coastline per year (Kempema et al., 1989), which is roughly twice the amount exported out of the shallow shelf zone by the ice field sampled in 2002. Riverine input of sediments from the Kuparuk and Colville drainage basins to the central Beaufort shelf amounts to 740,000 t $year^{-1}$ according to Reimnitz et al. (1988) as compared with higher estimates on the order of 6×10^6 t $year^{-1}$ by Milliman and Meade (1983). While the ice loads are much smaller than input from the Mackenzie river (124×10^6 t $year^{-1}$, Macdonald et al., 2003), ice export of sediments nevertheless plays a role in the Mackenzie shelf budget, in particular as it provides for a very rapid transport mechanism towards the west, directed against the coastal current (Weingartner et al., 1998; Carmack and Macdonald, 2002).

As indicated by the buoy drift both prior and subsequent to the sampling campaign in May/June 2002, the ice-transported sediments were conveyed from the eastern Chukchi and various locations along the entire Beaufort shelf into the western Chukchi Sea and the adjacent Arctic Ocean (Fig. 6). This overall drift pattern is commensurate with the long-term mean ice motion in this sector of the Arctic, which follows the anticyclonic Beaufort Gyre with a velocity on the order of 2.8 km day^{-1} (Rigor et al., 2002). This westward ice transport of sediments represents an important mode of particulate transfer, and to a lesser extent organic carbon (Macdonald et al., 2003; Eicken, 2003). Much of the sediment load is likely to be released in an area of high water column and benthic production (Naidu et al., 2003) based on typical ice drift velocities (Fig. 1; Rigor et al., 2002). Off- and cross-shelf transports are more difficult to assess, in particular as they impact ice transport of material into the deeper basins. Changes in ice circulation patterns (Tucker et al., 2001; Rigor et al., 2002), increase the likelihood of northward advection of sediment-laden ice, while changes in ice extent and concentration (Comiso, 2002) may enhance melting and release of sediments over the same area. Considering that the present study, observations of a single comparable event (Reimnitz et al., 1993b), as well as other reports of similar types of sediment-laden ice

in the Chukchi/Beaufort Sea shelf regions (Kempema et al., 1989; Tucker et al., 1999; Melling, unpublished observations, 2003), suggest potentially much higher transport of particulate matter by sea ice than generally acknowledged (see discussion in Eicken, 2003, and below), a more systematic study of ice-transport of sediments may be required.

4.3. *Are sediment entrainment and export from the Beaufort and Chukchi shelves increasing in importance due to a changing sea-ice regime?*

The consensus of work up to the present appears to be that sediment entrainment into sea ice over the Beaufort and Chukchi shelves and subsequent export is an interesting and locally important phenomenon, but is not as relevant for large-scale Arctic sediment transport as similar processes occurring over the vast, shallow Siberian shelves (Larssen et al., 1987; Nürnberg et al., 1994; Reimnitz et al., 1994; Pfirman et al., 1997; Nørgaard-Pedersen et al., 1998; Behrends, 1999; Eicken, 2003). A significant entrainment and export event in the Beaufort Sea in the winter of 1989 (with similarities to the ice studied here, though observed over a smaller area) was considered abnormal by Reimnitz et al. (1993b). The only other event of sediment entrainment at this scale for the region was reported by Kempema et al. (1989) for the Beaufort Sea offshore of Simpson Lagoon, where sediment load in some areas was estimated as high as $1000\,t\,km^{-2}$. A study of ice trajectories and sediment composition by Pfirman et al. (1997) pointed towards the central Siberian shelves as key entrainment areas. A detailed examination of a single entrainment event off the New Siberian Islands yielded sediment loads in Siberian drift ice exported into the Arctic Ocean and Greenland Sea far surpassing numbers published for the North American Arctic (Eicken et al., 2000). It is at present unclear how the finding by Darby (2003) of the Banks Island shelf as an important sediment entrainment and source area fits in with the observations of this study. Nevertheless, his study is a notable exception in that it assigns basinwide importance to this shelf area, based on the analysis of ice-transported materials' mineralogical composition.

Considering that the Chukchi and Beaufort Seas have seen the most significant sea-ice changes in the Arctic during the 1990s as compared to the previous two decades, increased entrainment and export of sediment-laden ice may be a result of environmental variability and change. This is supported by comparable observations of sediment-laden ice in the study area by one of us in 2003 (H. Melling, unpublished observations) as well as an increase in sediment entrainment into coastal lagoons near Barrow during the past seven winters as compared to earlier years (Stierle and Eicken, 2002; Shapiro, pers. comm.). Furthermore, Tucker et al. (1999) found some of the highest particulate loadings throughout their trans-Arctic sampling campaign in sea ice originating from the Chukchi Sea (their sites 207 and 208, Tucker et al., 1999).

The likelihood of resuspension of sediments during fall freeze-up and in winter has greatly increased since the late 1980s and early 1990s through a combination of several factors. First, fall and winter storms have become more frequent and stronger in the western Arctic (Serreze et al., 2000). Second, the amount of fetch has increased by up to an order of magnitude with a far northward retreat of the summer minimum ice edge (Comiso, 2002; Drobot and Maslanik, 2003). In the absence of wave height data, it nevertheless appears reasonable to assume up to a doubling of extreme wave heights. Third, due to increased summer melt and changes in the circulation regime (Tucker et al., 2001), thin first-year ice has almost entirely displaced multi-year ice over the Beaufort and northern Chukchi shelves. In combination with increases in storminess, this latter change could result in a more mobile ice cover and increased flaw lead openings, if first-year ice accommodates offshore motion more easily through rafting and ridging than multi-year ice. At present, we are lacking suitable data and more detailed analyses to resolve this issue. The Doppler sonar-derived ice velocities from the Mackenzie shelf do not indicate any significant trend in ice drift speed or tortuosity between 1990 and 2001, but the high temporal variations in ice velocity and the larger-scale configuration of the coastline in the Mackenzie region may render conclusions for the whole of the Alaska coastline difficult. The stratigraphic analysis and growth history of the ice observed in this study as well as in that of Reimnitz et al. (1993b) are certainly indicative of a highly dynamic ice environment with convergence and divergence of thin sea ice in the coastal regions punctuated by frazil formation and sediment entrainment events. This is corroborated by analyses of ice deformation from sequences of Radarsat SAR, which show some of the highest rates of shear

and vorticity in the first-year ice of the Beaufort and Chukchi Seas (Richter-Menge et al., 2002b). Iñupiat Eskimo in coastal villages also comment on a more dynamic ice cover under less stable and stormier weather conditions (Shapiro and Metzner, 1979; Krupnik and Jolly, 2002).

Potentially linked to these large-scale changes are increased occurrences of wintertime landfast ice break-out events, which expose broader stretches of shallow water. This greatly increases the likelihood of frazil formation and sediment entrainment. At Barrow, such events have occurred almost yearly during the past decade. One such event as observed by Radarsat SAR in December 2001 is shown in Fig. 12. As in this case, the strong offshore winds leading to the detachment of the shorefast ice also promote wind mixing and the seaward export of sediment-laden frazil ice. Similar to the larger polynya opened up in February 2002 (Fig. 8), this smaller episode will have contributed to the total sediment load observed in the study area. With comparatively few areas sufficiently shallow for sediment entrainment outside the landfast ice edge (Fig. 10, Table 2), winter ice break-out is important. Once the landfast ice edge is stable at 20–25 m water depth (Figs. 9 and 10; Tucker et al., 1979; Shapiro and Barnes, 1991; Dmitrenko et al., 1999), sediment entrainment over the broad shallow Siberian and narrow North American Arctic shelves may be quite comparable throughout winter. With fall storminess, fetch and winter ice break-out events increasing, ice transport may become quantitatively more important in the western Arctic, in particular if the observed changes in sea-ice and atmospheric conditions are part of a continuing trend.

The fate of sediment-laden ice and in particular the locations of sediment release from melting ice are also strongly dependent on the ice regime and in particular the atmospheric circulation regime. The drop in Arctic sea-level pressure in the 1990s has weakened the Beaufort Gyre, reducing westward ice velocities in the Chukchi and Beaufort Seas by more

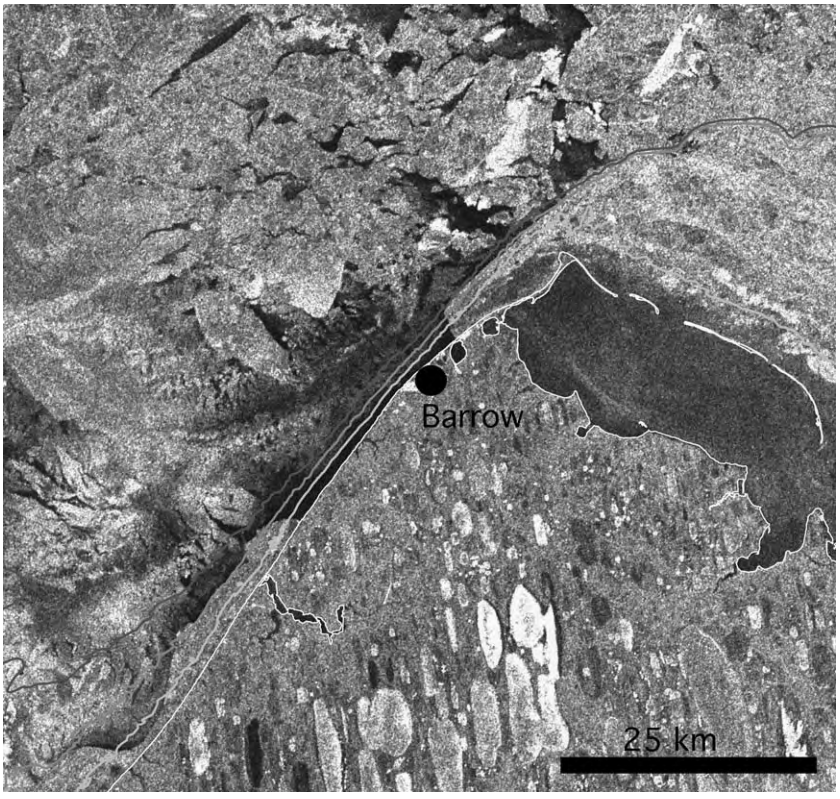

Fig. 12. Radarsat SAR scene of landfast ice break-out event (scene from December 13, 2001, 2 days after break-out; © Canadian Space Agency), showing the complete removal of landfast ice over a stretch of approximately 25 km of the coastline starting at just northeast of the village of Barrow. The 10-m, 20-m and 30-m depth contours from the NOS bathymetry are also shown. Open water and thin new ice near the coast appear dark due to low radar backscatter, while thicker, rough landfast ice and older ice floating offshore appear in lighter shades of gray.

than a third (Rigor et al., 2002). In conjunction with other shifts in the ice regime (Tucker et al., 2001), this change appears to have increased the flux of ice and its sediment load into the central Arctic.

Increased sediment entrainment has a number of important implications in the context of shelf–basin interactions. Thus, even smaller concentrations of sediments in sea ice have been shown to significantly affect the amount of light penetrating into the water column and the lower ice layers (Light et al., 1998), with substantial impacts on primary production in the ice and water column (Dunton, 1985; Grossmann and Gleitz, pers. comm., 1995; Gradinger et al., submitted). In a study of ice-associated flora and fauna in clean and sediment-laden coastal ice (with sediment loads of 106 t km^{-2} comparable to those found offshore), Gradinger et al. (submitted) found a reduction of algal biomass by a factor of 30 and associated decreases in abundance of metazoans. Such negative impacts on primary production can cascade up through the higher trophic levels of the food web. The impact on the highly productive Chukchi Sea ecosystem, with some of the highest levels of ice algal biomass and benthic biomass found anywhere in the Arctic (Naidu et al., 2003; Gradinger et al., in prep.) could be particularly severe. Furthermore, ice transport of sediments can rapidly transport pollutants deposited with sediments in shallow water to the deeper shelf and basins (Lange and Pfirman, 1998; Macdonald et al., 2000). Increasing offshore oil and gas development in the Alaskan and Canadian Arctic is likely to increase both the level of continuous low-level pollutant discharge into the environment as well as the likelihood of a catastrophic release during an oil spill (Atlas, 1979; Macdonald et al., 2000). Mobilization of pollutants accumulating over decades in shallow-water environments in association with sediment transport may result in their direct transfer to benthic communities and higher trophic levels. At the same time, it needs to be assessed to what an extent oil released in under-ice or open-water environments can be entrained into the ice cover jointly with resuspended sediments. Coagulation and compression of such oil–particle mixtures during ice ageing (Goldschmidt et al., 1992; Stierle and Eicken, 2002) and the subsequent release from landfast or drifting ice could convey oil directly into the sediment layer where the potential impact on the Chukchi and Beaufort ecosystems with their dependence on benthic biomass is high.

5. Summary and conclusions

Field observations revealed the wide-spread occurrence of sediment-laden sea ice over the eastern Chukchi and western Beaufort Sea shelves in late spring of 2002. With an average load of 128 t km^{-2} over $>100{,}000$ km^2, the $>4\times10^6$ t of particulates (and 1–3% organic carbon typically associated with western Arctic shelf sediments) transported with the ice contribute substantially to the shelf's sediment and carbon budget. Of particular importance is the westward trend of this flux, into the high-productivity areas of the Chukchi Sea. The impact of this ice-associated transport on Chukchi and Beaufort Sea ecosystems is complex and as of yet largely unexplored. The comparatively minor benefits extended to benthic communities by the additional input of organic carbon may well be offset by the potential for pollutant transfer from shallow-water environments in areas of on- and offshore oil and gas development. Most important, however, is the potentially substantial reduction in (sub-) ice algal primary production, which has been shown to reduce algal standing stock by more than a factor of 30, with corresponding impacts on metazoan populations (Gradinger et al., submitted).

The high sediment concentrations found mostly in the lower layers of the ice contrast with observations of sediment-laden ice in coastal lagoons and the Laptev Sea. Ice stratigraphy and inferences about ice growth obtained from satellite data and a simple growth model suggest that this distribution is due to sediment entrainment into frazil ice in a dynamic coastal polynya environment. This distribution of sediments within the ice column renders mapping of sediments with remote-sensing techniques during the melt season difficult and leads to an underestimation of sediment distribution in ship-based and airborne observations.

The origins of the sediment-laden ice could be traced back through a combination of ice-drift data (from buoys and Doppler Sonar), ice-core analysis and remote-sensing data. Two distinct entrainment regions emerged, with a large polynya opening in the eastern Chukchi Sea between Barrow and Icy Cape in early February 2002. The comparatively large area of water shallow enough for entrainment of sediments in conjunction with landfast ice breakout events that exposed shallow water all the way to the beach to the newly forming ice cover account for efficient entrainment and export of sediments into the offshore Chukchi Sea. With the shallow water

areas outside of the landfast ice edge, sediment-laden ice appears to have formed in a number of locations along the entire Beaufort coast. The Mackenzie shelf constitutes the most extensive shallow-water environment (both prior to and after landfast ice formation), and even with an overall reduction in westward ice drift as a result of large-scale circulation changes (Rigor et al., 2002), ice formed over the Mackenzie shelf during freeze-up in mid-October reached the easternmost stretches of the study area. Additional input of ice must have occurred in the central and western Beaufort Sea, where the landfast ice edge exposed shallow water during the course of the winter. However, based on analysis of wave heights and orbital speeds at one of the moored sonar sites, standard resuspension models suggest that little if any resuspension of sediment occurs during polynya and lead openings by wave action alone. It is presently not clear whether (tidal) currents or the interaction of ice crystals with the seafloor can explain sediment entrainment under such conditions.

Changes in the large-scale sea-ice regime offer one possible explanation for increasing observations of sediment-laden ice in the Beaufort and Chukchi Seas. While one also has to consider the introduction of bias due to increased and better sampling in recent years, observations and theoretical considerations suggest that sediment-laden ice may contribute more significantly to shelf sediment dynamics if the observed changes in ice conditions are part of a long-term trend. Specifically mid-winter landfast ice break-out events could dramatically increase sediment export.

The study of sediment transport by sea ice remains plagued by the episodic and localized nature of entrainment and export events. Remote sensing may be hampered by confinement of sediments to the lower ice layers underneath up to a meter or more of clean ice, as observed here. Hence, it may require a more concerted observation and monitoring effort that combines ice sampling, remote sensing (including deployment of underwater sensors to detect sediments through their modification of ice optical properties) and modeling at key locations.

Acknowledgments

We thank personnel onboard USCGC Healy for their professional and friendly support, their "can do" attitude helped considerably in assembling this data set. This work is supported by NSF Grant OPP-0125464 as part of the Shelf–Basin Interactions Program. Alaska Satellite Facility personnel provided help with processing of Radarsat SAR data, which were obtained through a NASA-ADRO2 Grant. Thanks go to Jackie Grebmeier for all her efforts as part of the SBI Program that made this research possible. Supplemental funding came from the Minerals Management Service Contract 71707. Michael Tapp was a great help in the field and the lab, Marc Webber helped with ice observations and Patrick Cotter assembled some of the maps. Stable isotope data were provided by Gordon Bower and Nori Tanaka. Barrow Arctic Science Consortium (BASC) provided logistics support for measurements in Barrow. Two anonymous reviewers, Lars Henrik Smedsrud, Lew Shapiro and Erk Reimnitz provided helpful comments on how to improve the manuscript. Thank you!

References

Ackermann, N.L., Shen, H.T., Sanders, B., 1994. Experimental studies of sediment enrichment of arctic ice covers due to wave action and frazil entrainment. Journal of Geophysical Research 99, 7761–7770.

Atlas, R.M., 1979. Assessment of potential interactions of microorganisms and pollutants resulting from petroleum development on the outer continental shelf of Alaska: environmental assessment of the Alaskan continental shelf. Annual Reports of Principal Investigators for the Year ending March 1979, vol. 5, Receptros—Microbiology, Contaminant Baselines. NOAA/ERL, Boulder, CO (USA), pp. 1–61.

Barnes, P.W., Reimnitz, E., Fox, D., 1982. Ice rafting of fine-grained sediment, a sorting and transport mechanism, Beaufort Sea, Alaska. Journal of Sedimentary Petrology 52, 493–502.

Behrends, M., 1999. Reconstruction of sea-ice drift and terrigenous sediment supply in the Late Quaternary: heavy-mineral associations in sediments of the Laptev-Sea continental margin and the central Arctic Ocean. Berichte zur Polarforschung 310, 1–167 (in German).

Bischof, J.F., Darby, D.A., 1997. Mid- to late Pleistocene ice drift in the western Arctic Ocean: evidence for a different circulation in the past. Science 277, 74–84.

Carmack, E.C., Macdonald, R.W., 2002. Oceanography of the Canadian shelf of the Beaufort Sea: a setting for marine life. Arctic 55, 29–45.

Clark, D.L., Hanson, A., 1983. Central Arctic Ocean sediment texture: a key to ice transport mechanisms. In: Molnia, B.F. (Ed.), Glacial-Marine Sedimentation. Plenum Press, New York, pp. 301–330.

Comiso, J.C., 2002. A rapidly declining perennial sea ice cover in the Arctic. Geophysical Research Letters 29, 1956 [doi:10.1029/2002GL015650].

Cooper, L.W., Whitledge, T.E., Grebmeier, J.M., Weingartner, T., 1997. The nutrient, salinity, and stable oxygen isotope composition of Bering and Chukchi Seas waters in and near the Bering Strait. Journal of Geophysical Research 102, 12563–12573.

Darby, D.A., 2003. Sources of sediment found in sea ice from the western Arctic Ocean, new insights into processes of entrainment and drift patterns. Journal of Geophysical Research 108, 3257 [doi:10.1029/2002JC001350].

Dethleff, D., Nürnberg, D., Reimnitz, E., Saarso, M., Savchenko, Y.P., 1993. East Siberian Arctic Region Expedition '92: the Laptev Sea—its significance for Arctic sea ice formation and transpolar sediment flux. Berichte zur Polarforschung 120, 3–37.

Dethleff, D., Loewe, P., Kleine, E., 1998. The Laptev Sea flaw lead—detailed investigation on ice formation and export during 1991/92 winter season. Cold Regions Science and Technology 27, 225–243.

Dmitrenko, I.A., Gribanov, V.A., Volkov, D.L., Kassens, H., Eicken, H., 1999. Impact of river discharge on the fast ice extension in the Russian Arctic shelf area. In: Proceedings of the 15th International Conference on Port and Ocean Engineering under Arctic Conditions (POAC99), Helsinki, 23–27 August, 1999, vol. 1, pp. 311–321.

Drobot, S.D., Maslanik, J.A., 2003. Interannual variability in summer Beaufort Sea ice conditions: relationship to winter and summer surface and atmospheric variability. Journal of Geophysical Research 108, 3233 [doi:10.1029/2002JC001537].

Dunton, K.H., 1985. Growth of dark-exposed *Laminaria saccharina* (L.) Lamour and *Laminaria solidungula* J. Ag. (Laminariales: Phaeophyta) in the Alaskan Beaufort Sea. Journal of Experimental Marine Biology and Ecology 94, 181–189.

Eicken, H., 2003. The role of Arctic sea ice in transporting and cycling terrigenous organic matter. In: Stein, R., Macdonald, R.W. (Eds.), The Organic Carbon Cycle in the Arctic Ocean. Springer, Berlin, pp. 45–53.

Eicken, H., Lange, M.A., 1989. Development and properties of sea ice in the coastal regime of the southeastern Weddell Sea. Journal of Geophysical Research 94, 8193–8206.

Eicken, H., Reimnitz, E., Alexandrov, V., Martin, T., Kassens, H., Viehoff, T., 1997. Sea-ice processes in the Laptev Sea and their importance for sediment export. Continental Shelf Research 17, 205–233.

Eicken, H., Kolatschek, J., Freitag, J., Lindemann, F., Kassens, H., Dmitrenko, I., 2000. Identifying a major source area and constraints on entrainment for basin-scale sediment transport by Arctic sea ice. Geophysical Research Letters 27, 1919–1922.

Eicken, H., Tucker, W.B.I., Perovich, D.K., 2001. Indirect measurements of the mass balance of summer Arctic sea ice with an electromagnetic induction technique. Annals of Glaciology 33, 194–200.

Eicken, H., Krouse, H.R., Kadko, D., Perovich, D.K., 2002. Tracer studies of pathways and rates of meltwater transport through Arctic summer sea ice. Journal of Geophysical Research 107 [doi:10.1029/2000JC000583].

Frey, K., Eicken, H., Perovich, D.K., Grenfell, T.C., Light, B., Shapiro, L.H., Stierle, A.P., 2001. Heat budget and decay of clean and sediment-laden sea ice off the northern coast of Alaska. In: Port and Ocean Engineering in the Arctic Conference (POAC'01) Proceedings, vol. 3, Ottawa, Canada, pp. 1405–1412.

Galloway, J.L., Melling, H., 1997. Tracking the motion of sea ice by correlation sonar. Journal of Atmospheric and Oceanic Technology 14, 616–629.

Goldschmidt, P.M., Pfirman, S.L., Wollenburg, I., Henrich, R., 1992. Origin of sediment pellets from the arctic seafloor: sea ice or icebergs? Deep-Sea Research II 39, S539–S565.

Gradinger, R.R., Bluhm, B.A., Nielsen, M.R. The pivotal role of sea ice sediments for the seasonal development of near-shore Arctic fast ice biota off Barrow, Alaska. Marine Ecology Progress Series, submitted for publication.

Haas, C., Eicken, H., 2001. Interannual variability of summer sea ice thickness in the Siberian and Central Arctic under different atmospheric circulation regimes. Journal of Geophysical Research 106, 4449–4462.

Huck, P., Light, B., Eicken, H. Mapping sediment-laden sea ice in the Arctic using AVHRR remote-sensing data: atmospheric correction and determination of reflectances as a function of ice type and sediment load. Remote Sensing of the Environment, submitted for publication.

Junge, K., Eicken, H., Deming, J.W., 2004. Bacterial activity at −2 to −20 °C in Arctic wintertime sea ice. Applied Environmental Microbiology 70, 550–557.

Kempema, E.W., Reimnitz, E., Barnes, P.W., 1989. Sea ice sediment entrainment and rafting in the Arctic. Journal of Sedimentary Petrology 59, 308–317.

Komar, P.D., Miller, M.C., 1973. The threshold of sediment movement under oscillatory water waves. Journal of Sedimentary Petrology 43, 1101–1110.

Krupnik, I., Jolly, D., 2002. The Earth is Faster Now: Indigenous Observations of Arctic Environmental Change, Arctic Research Consortium of the United States, Fairbanks, Alaska.

Lange, M.A., Pfirman, S.L., 1998. Arctic sea ice contamination: major characteristics and consequences. In: Leppäranta, M. (Ed.), Physics of Ice-covered Seas, 2. University of Helsinki, Helsinki, pp. 651–681.

Larssen, B.B., Elverhøi, A., Aagaard, P., 1987. Study of particulate material in sea ice in the Fram Strait—a contribution to paleoclimatic research? Polar Research 5, 313–315.

Light, B., Eicken, H., Maykut, G.A., Grenfell, T.C., 1998. The effect of included particulates on the optical properties of sea ice. Journal of Geophysical Research 103, 27739–27752.

Lindemann, F., 1999. Sediments in Arctic sea ice—entrainment, characterization and quantification. Berichte zur Polarforschung 283, 1–124 (in German).

Macdonald, R.W., Paton, D.W., Carmack, E.C., Omstedt, A., 1995. The freshwater budget and under-ice spreading of Mackenzie River water in the Canadian Beaufort Sea based on salinity and $^{18}O/^{16}O$ measurements in water. Journal of Geophysical Research 100, 895–919.

Macdonald, R.W., Solomon, S.M., Cranston, R.E., Welch, H.E., Yunker, M.B., Gobeil, C., 1998. A sediment and organic carbon budget for the Canadian Beaufort Shelf. Marine Geology 144, 255–273.

Macdonald, R.W., Carmack, E.C., Paton, D.W., 1999. Using the $\delta^{18}O$ composition in landfast ice as a record of arctic estuarine processes. Marine Chemistry 65, 3–24.

Macdonald, R.W., et al., 2000. Contaminants in the Canadian Arctic: 5 years of progress in understanding sources,

occurrences and pathways. The Science of the Total Environment 254, 93–234.

Macdonald, R.W., Naidu, A.S., Yunker, M.B., Gobeil, C., 2003. The Beaufort Sea: distribution, sources, fluxes and burial of organic carbon. In: Stein, R., Macdonald, R.W. (Eds.), The Organic Carbon Cycle in the Arctic Ocean. Springer, Berlin, pp. 177–193.

Melling, H., Moore, R.M., 1995. Modification of halocline source waters during freezing on the Beaufort Sea shelf: evidence from oxygen isotopes and dissolved nutrients. Continental Shelf Research 15, 89–113.

Melling, H., Johnston, P.H., Riedel, D.A., 1995. Measurement of the underside topography of sea ice by moored subsea sonar. Journal of Atmospheric and Oceanic Technology 12, 589–602.

Milliman, J.D., Meade, R.H., 1983. World-wide delivery of river sediment to the oceans. Journal of Geology 91, 1–21.

Naidu, A.S., Cooper, L.W., Grebmeier, J.M., Whitledge, T.E., Hameedi, M.J., 2003. The continental margin of the North Bering–Chukchi Sea: concentrations, sources, fluxes, accumulation and burial rates of organic carbon. In: Stein, R., Macdonald, R.W. (Eds.), The Organic Carbon Cycle in the Arctic Ocean. Springer, Berlin, pp. 193–203.

Nørgaard-Pedersen, N., Spielhagen, R.F., Thiede, J., Kassens, H., 1998. Central Arctic surface ocean environment during the past 80,000 years. Paleoceanography 13, 193–204.

Nürnberg, D., Wollenburg, I., Dethleff, D., Eicken, H., Kassens, H., Letzig, T., Reimnitz, E., Thiede, J., 1994. Sediments in Arctic sea ice—implications for entrainment, transport and release. Marine Geology 119, 185–214.

Osterkamp, T.E., Gosink, J.P., 1984. Observations and analyses of sediment-laden sea ice. In: Barnes, P.W., Schell, D.M., Reimnitz, E. (Eds.), The Alaskan Beaufort Sea: ecosystems and environments. Academic Press, Orlando, pp. 73–93.

Perovich, D.K., Grenfell, T.C., Eicken, H., Richter-Menge, J.A., Sturm, M., Ligett, K., Frey, K., Maykut, G.A., Elder, B., Mahoney, A., Holmgren, J., Claffey, K., 2001. Arctic Coastal Processes Data Report 2001. CD-ROM.

Perovich, D.K., Grenfell, T.C., Richter-Menge, J.A., Light, B., Tucker III, W.B., Eicken, H., 2003. Thin and thinner: Sea ice mass balance measurements during SHEBA. Journal of Geophysical Research 108, 99 [doi:10.1029/2001JC001079].

Pfirman, S., Colony, R., Nürnberg, D., Eicken, H., Rigor, I., 1997. Reconstructing the origin and trajectory of drifting Arctic sea ice. Journal of Geophysical Research 102, 12575–12586.

Pfirman, S., Wollenburg, I., Thiede, J., Lange, M.A., 1989. Lithogenic sediment on Arctic pack ice: potential aeolian flux and contribution to deep sea sediments. In: Leinen, M., Sarnthein, M. (Eds.), Paleoclimatology and paleometeorology: modern and past patterns of global atmospheric transport. Kluwer Academic Publishers (NATO ASI C282), Dordrecht, pp. 463–493.

Pfirman, S., Lange, M.A., Wollenburg, I., Schlosser, P., 1990. Sea ice characteristics and the role of sediment inclusions in deep-sea deposition: Arctic–Antarctic comparisons. In: Bleil, U., Thiede, J. (Eds.), Geological history of the Polar Oceans: Arctic versus Antarctic. Kluwer Academic Publishers, Dordrecht, pp. 187–211.

Reimnitz, E., Kempema, E.W., Barnes, P.W., 1987. Anchor ice, seabed freezing, and sediment dynamics in shallow arctic seas. Journal of Geophysical Research 92, 14671–14678.

Reimnitz, E., Graves, S.M., Barnes, P.W., 1988. Map showing Beaufort Sea coastal erosion, sediment flux, shoreline evolution, and the erosional shelf profile, US G. S. Miscellaneous Investigation Series, Map I-1182 G.

Reimnitz, E., Barnes, P.W., Weber, W.S., 1993a. Particulate matter in pack ice of the Beaufort Gyre. Journal of Glaciology 39, 186–198.

Reimnitz, E., McCormick, M., McDougall, K., Brouwers, E., 1993b. Sediment export by ice rafting from a coastal polynya, Arctic Alaska, USA. Arctic, Antarctic and Alpine Research 25, 83–98.

Reimnitz, E., Clayton, J.R., Kempema, E.W., Payne, J.R., Weber, W.S., 1993c. Interaction of rising frazil with suspended particles: tank experiments with applications of nature. Cold Regions Science and Technology 21, 117–135.

Reimnitz, E., Dethleff, D., Nürnberg, D., 1994. Contrasts in Arctic shelf sea-ice regimes and some implications: Beaufort Sea and Laptev Sea. Marine Geology 119, 215–225.

Richter-Menge, J., Elder, B., Claffey, K., Overland, J., Salo, S., 2002a. In situ sea ice stresses in the western Arctic during the winter of 2001–2001. In: Squire, V., Langhorne, P. Ed. (Eds.), Ice in the Environment: Proceedings of the 16th IAHR International Symposium on Ice, December 2–10, 2002, vol. 2: International Association of Hydraulic Engineering and Research, Dunedin, New Zealand, pp. 423–430.

Richter-Menge, J.A., McNutt, S.L., Overland, J.E., Kwok, R., 2002b. Relating arctic pack ice stress and deformation under winter conditions. Journal of Geophysical Research 107, 8040 [doi:10.1029/2000JC000477].

Rigor, I.G., Wallace, J.M., Colony, R.L., 2002. Response of sea ice to the Arctic Oscillation. Journal of Climate 15, 2648–2663.

Serreze, M.C., Walsh, J.E., Chapin III, F.S., Osterkamp, T., Dyurgerov, M., Romanovsky, V., Oechel, W.C., Morison, J., Zhang, T., Barry, R.G., 2000. Observational evidence of recent change in the northern high-latitude environment. Climatic Change 46, 159–207.

Shapiro, L.H., Barnes, P.W., 1991. Correlation of nearshore ice movement with seabed ice gouges near Barrow, Alaska. Journal of Geophysical Research 96, 16979–16989.

Shapiro, L.H., Metzner, R.C., 1979. Historical references to ice conditions along the Beaufort Sea coast of Alaska. University of Alaska, Geophysical Institute, Scientific Report.

Sherwood, C.R., 2000. Numerical model of frazil ice and suspended sediment concentrations and formation of sediment laden ice in the Kara Sea. Journal of Geophysical Research 105, 14061–14080.

Smedsrud, L.H., 2001. Frazil-ice entrainment of sediment: large-tank laboratory experiments. Journal of Glaciology 47, 461–471.

Smedsrud, L.H., 2002. A model for entrainment of sediment into sea ice by aggregation between frazil-ice crystals and sediment grains. Journal of Glaciology 48, 51–61.

Smedsrud, L.H., 2003. Formation of turbid ice during autumn freeze up in the Kara Sea. Polar Research 22, 267–286.

Stierle, A.P., Eicken, H., 2002. Sedimentary inclusions in Alaskan coastal sea ice: small-scale distribution, interannual variability and entrainment requirements. Arctic, Antarctic and Alpine Research 34, 103–114.

Stringer, W.J., 1978. Morphology of Beaufort, Chukchi and Bering Seas nearshore ice conditions by means of satellite and aerial remote sensing, environmental assessment of the

Alaskan continental shelf, vol.10: Transport. Principal Investigators' Annual Reports for the year ending March 1978, Outer Continental Shelf Environmental Assessment Program, Boulder, Colorado, pp. 1–220.

Toyota, T., Kawamura, T., Ohshima, K.I., Shimoda, H., Wakatsuchi, M., 2004. Thickness distribution, texture, and stratigraphy, and a simple probabilistic model for dynamical thickening of sea ice in the Southern Okhotsk Sea. Journal of Geophysical Research 109, C06001 [doi:10.1029/2003JC002090].

Tucker, W.B., Weeks, W.F., Frank, M., 1979. Sea ice ridging over the Alaska continental shelf. Journal of Geophysical Research 84, 4885–4897.

Tucker III, W.B., Gow, A.J., Meese, D.A., Bosworth, H.W., Reimnitz, E., 1999. Physical characteristics of summer ice across the Arctic Ocean. Journal of Geophysical Research 104, 1489–1504.

Tucker, W.B.I., Weatherly, J.W., Eppler, D.T., Farmer, D., Bentley, D.L., 2001. Evidence for the rapid thinning of sea ice in the western Arctic Ocean at the end of the 1980s. Geophysical Research Letters 28, 2851–2854.

Untersteiner, N., 1968. Natural desalination and equilibrium salinity profile of perennial sea ice. Journal of Geophysical Research 73, 1251–1257.

Warren, S.G., 1984. Impurities in snow: effects on albedo and snowmelt. Annals of Glaciology 5, 177–179.

Weingartner, T.J., Cavalieri, D.J., Aagaard, K., Sasaki, Y., 1998. Circulation, dense water formation, and outflow on the northeast Chukchi shelf. Journal of Geophysical Research 103, 7647–7661.